

MODELLING AND OPTIMIZATION OF  
COMPACT SUBSEA SEPARATORS

FAHAD MATOVU

December 9, 2014

## **Abstract**

This report is a part of the Master thesis, Modelling and optimization of a compact subsea separation system. The project work starts by considering the compact separation system by Christian Ellingsen (Ellingsen, 2007). The separation system consists of 3 separation units; a gravity separator, a deliquidizer and a degasser.

The initial work done has been focused on modelling of the deliquidizer, a unit that separates liquid from the bulk gas that exits the gravity separator. The modelling of separation in the main section of this unit has been based on simple concepts of radial settling velocity, time of flight model and uniform droplet distribution resulting in prediction of gas volume fractions of the exiting stream. Modelling of separation in the boot section of the deliquidizer has not yet been done.

The model results obtained are compared to two experimental data sets where performance is on average okay despite some short comings, and with some model improvements, better performance is expected.

A continuation of this work is to be done in the spring semester 2015, with the modelling of the other units and optimization expected to be done.

## **Acknowledgement**

I would like to extend my sincere thanks to my supervisors Johannes Jäschke and Sigurd Skogestad for their technical knowledge, support and guidance in this project work.

It has not been an easy task to accomplish the aims of this work especially due to my technical inexperience in this field of study as well as the challenging access to information related to subsea separation technologies as far as I have been concerned.

However, I am glad that I have been able to present something that seems quite encouraging in this report. Thank you all.

## List of Tables

1	Parameters . . . . .	24
---	----------------------	----

## List of Figures

1	Compact separation system . . . . .	7
2	Vertical three phase separator . . . . .	9
3	Typical inline deliquidizer . . . . .	10
4	Typical inline degasser . . . . .	12
5	Trajectory of droplet experiencing a centrifugal force . . . . .	16
6	Re-entrainment mechanisms . . . . .	21
7	Occurrence of re-entrainment . . . . .	23
8	Power function of $w$ against $Q_i$ . . . . .	25
9	Gompertz function of $w$ against $Q_i$ . . . . .	26
10	Model results for Power function . . . . .	26
11	Model results for Gompertz function . . . . .	27
12	Masked data for comparison . . . . .	28
13	Comparison of model results to data . . . . .	29
14	Comparison for corrected angular velocities . . . . .	29

# Contents

<b>Abstract</b>	<b>i</b>
<b>Acknowledgement</b>	<b>ii</b>
<b>List of Tables</b>	<b>iii</b>
<b>List of Figures</b>	<b>iii</b>
<b>1 INTRODUCTION</b>	<b>3</b>
1.1 Overview . . . . .	3
1.2 Motivation for compact separation technology . . . . .	4
1.3 Challenges of compact separation technology . . . . .	5
<b>2 COMPACT SEPARATION SYSTEMS</b>	<b>6</b>
2.1 Introduction . . . . .	6
2.2 Gravity separators . . . . .	8
2.3 Deliquidizer . . . . .	10
2.4 Degasser . . . . .	11
<b>3 MODELLING OF THE DELIQUIDIZER</b>	<b>13</b>
3.1 Modelling of separation in the main deliquidizer section . . .	13
3.1.1 Radial velocity . . . . .	13
3.1.2 Time of flight model . . . . .	15
3.1.3 Uniform droplet distribution . . . . .	18
3.1.4 Gas volume fraction . . . . .	18
3.2 Concepts for model improvement . . . . .	19
3.2.1 Modelling of swirl with decay . . . . .	19
3.2.2 Energy consumption . . . . .	20
3.2.3 Re-entrainment . . . . .	21
<b>4 RESULTS AND DISCUSSION</b>	<b>24</b>

<b>5 CONCLUSION AND FUTURE WORK</b>	<b>30</b>
5.1 Conclusion . . . . .	30
5.2 Future work . . . . .	30
<b>Bibliography</b>	<b>32</b>
<b>A Appendix</b>	<b>34</b>
A.1 gasfraction.m . . . . .	34
A.2 gasnew.m . . . . .	36

# 1 INTRODUCTION

## 1.1 Overview

The oil production industry is always faced with a challenge of separating oil well streams into component phases that include oil, water and gas, so as to process them into marketable products or dispose them off in a way that is environmentally friendly (Sayda and Taylor, 2007). In addition, it's also important to separate water and sand in the earliest production stages to prevent erosion and corrosion of production equipment (Swanborn, 1988).

The conventional separation techniques are usually costly, the equipment being of considerable size and weight thus affecting the space and load requirements, which greatly makes the processing facilities costly (Hamoud et al., 2009). Therefore efforts are in place to develop technologies for oil processing that limit the size and weight of process equipment in order to reduce cost and maximise the effectiveness of separation equipment. This has led to the emergency of compact inline separation systems.

These systems are at the moment at the highest level of separation technologies for both top-side and sub-sea separation. What makes them interesting is the fact that they minimize space and weight while optimizing separation efficiencies and there application in existing installations makes increased production possible (FMCtechnologies, 2011).

In inline separators, the separation is achieved by use of centrifugal force which is thousands of times greater than the force of gravity used in conventional separators (Hamoud et al., 2009). In contrast to conventional separators where fluids are allowed to have a few minutes of retention time under the influence of gravity, the need for long retention times in inline separators is eliminated. This is because the speed of separation is greatly increased in inline separators. The size of the separation vessels is in turn also greatly reduced (Hamoud et al., 2009).

## 1.2 Motivation for compact separation technology

The limited size and weight of compact separation technologies is very attractive because of limitation of space and load requirements thus reducing associated costs. The minimum weight and space requirements of these systems also help to make marginal fields commercially viable. Compact equipment can also be used in existing installations where space is limited to provide separation solutions that lead to increased production (FMCtechnologies, 2011).

Compact equipment can be installed top-side and sub-sea and due to the small size, these can be replaced according to specifications but only top-side as this opportunity does not present itself sub-sea. There also exists the possibility of changing the internals of the separation equipment previously installed.

Compact equipment are ideal for sub-sea separation and other high pressure applications since pressure vessels can be reduced in size, or sometimes even be eliminated when using inline separation equipment. The increased pressure sub-sea results in increased production of hydrocarbons.

Talking about sub-sea separation, it results in increased well productivity and therefore result in accelerated reservoir draining rates. It also reduces the requirement for high efficiency insulation systems especially in risk of formation of hydrates resulting in savings on cost and time required for insulation. Sub-sea separation also results in reduction in size, weight and associated cost of production water treatments installations top-side (Alary et al., 2000).

There are quite a number of benefits and advantages of using compact separation technologies especially sub-sea and that's why there is interest in carrying out this work.

### 1.3 Challenges of compact separation technology

However, there are also some potential draw backs. The small residence time associated with the compact separation equipment results in control challenges. The control of liquid and interface levels tends to be more challenging than in conventional separators since the former are more sensitive to flow variations. The small size also makes compact separation equipment difficult to operate.

Also, a potential problem with sub-sea separation is the impact of reduced liquid flow rate on flow behaviour which in a line may induce severe slugging. However, solutions to this problem such as the use of gas-lift in the riser exist (Alary et al., 2000). Also limited accessibility and high maintenance costs are challenges to sub-sea separation.

According to (Hamoud et al., 2009), the inline separation techniques utilizing centrifugal forces produce outlet streams with quality that is sufficient for practical purposes but may not as good as conventional separators.

## 2 COMPACT SEPARATION SYSTEMS

### 2.1 Introduction

The compact separation system used for this work is that according to (Ellingsen, 2007) as shown in figure 1 below.

As seen in figure 1, there are three separation units. The units discussed here are based on a new-inline technology where a centrifugal force is used to separate the phases because of their difference in densities. This separation system is compact because the units minimise space and weight and are designed to have almost the same dimensions as the transport pipe thus inline-technology (Ellingsen, 2007).

The gravity separator does the bulk separation of the gas and liquid phases that enter the unit. However, the separation obtained is not satisfactory as regards the demands of the compressor and pump. Therefore, the degasser and deliquidizer do further separation of the phases. The degasser separates gas from a liquid stream while the purpose of the deliquidizer is to separate liquid from a gas stream (FMCTechnologies, 2011). The modelling of the deliquidizer was the primary objective and therefore the principle of operation of the deliquidizer is discussed in detail in the subsequent sections of this report.

It's important to note about the compact separation system in figure 1 that the operational objective is to adjust the available valves in such a way that the gas content in the liquid stream is minimised. Therefore the quality of the liquid from the degasser is more important than the gas quality and therefore the gas phase from the degasser undergoes further separation in the deliquidizer.

It's also worth noting that the return streams of liquid and gas after the pump and compressor are not meant for use under normal operation. They are meant to ensure that there is enough feed to the pump and compressor

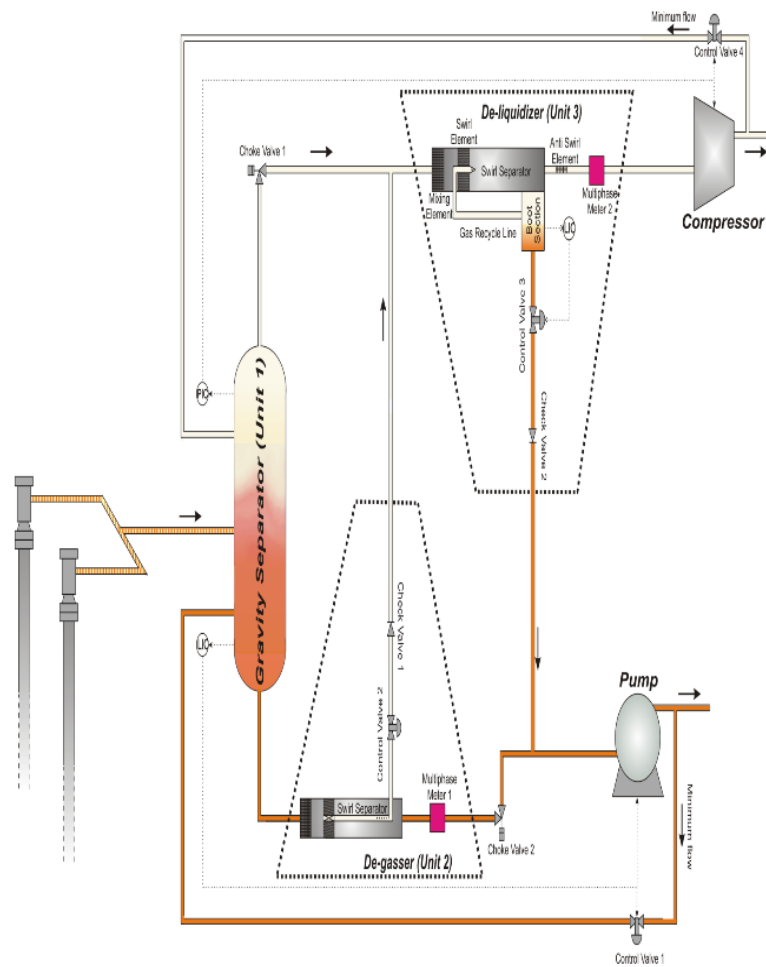


Figure 1: Compact separation system  
Adapted from (Ellingsen, 2007)

and that the flow rates through the deliquidizer and degasser are above certain limits (Ellingsen, 2007).

## 2.2 Gravity separators

These are pressure vessels that separate a mixed stream of liquid and gas phases into respective separate phases (Mokhatab and Poe, 2012). They employ the use of the gravity forces to separate the mixed phases based on their differences in density. The heavier phase settles at the bottom of the separator while the lightest rises to the top but this requires some settling time. The larger the difference in density, the higher the difference in velocity resulting in a lower settling time.

However, for large settling times, the separator need to be larger to effect the separation. Due to the fact that large separator vessel sizes are required to achieve settling, gravity separators are rarely designed to remove droplets smaller than 250  $\mu\text{m}$  (Mokhatab and Poe, 2012).

Gravity separators are often classified to be vertical or horizontal based on their geometrical configuration or by their function. For example, they are “two-phase” if they separate gas from a liquid stream (Mokhatab and Poe, 2012).

Let us briefly discuss some parts of a gravity separator and their role during separation. The figure 2 below is that of a vertical three phase separator for oil-water and gas adapted from (Mokhatab and Poe, 2012). The three phase stream enters through the side where the inlet divider separates the bulk of gas. The gas goes upwards through the mist extractor that captures the entrained liquid droplets and out through the gas outlet. The liquid moves downwards to the oil-water interface where oil and water separate by moving in counter-current directions to one another. Also, the oil droplets trapped in water rise in counter-current direction to water flow. The separated oil flows out through the oil outlet and water through the

water outlet at the bottom thus separating the phases (Mokhatab and Poe, 2012). The chimney is used to equalise the pressure between the gas section and lower section of the separator. An important point to note for a vertical separator is that level control is not critical, the liquid level can fluctuate slightly without affecting the efficiency. The forces that come into play for the separation to take place will be discussed in the subsequent sections in build up to modelling cyclonic separation units.

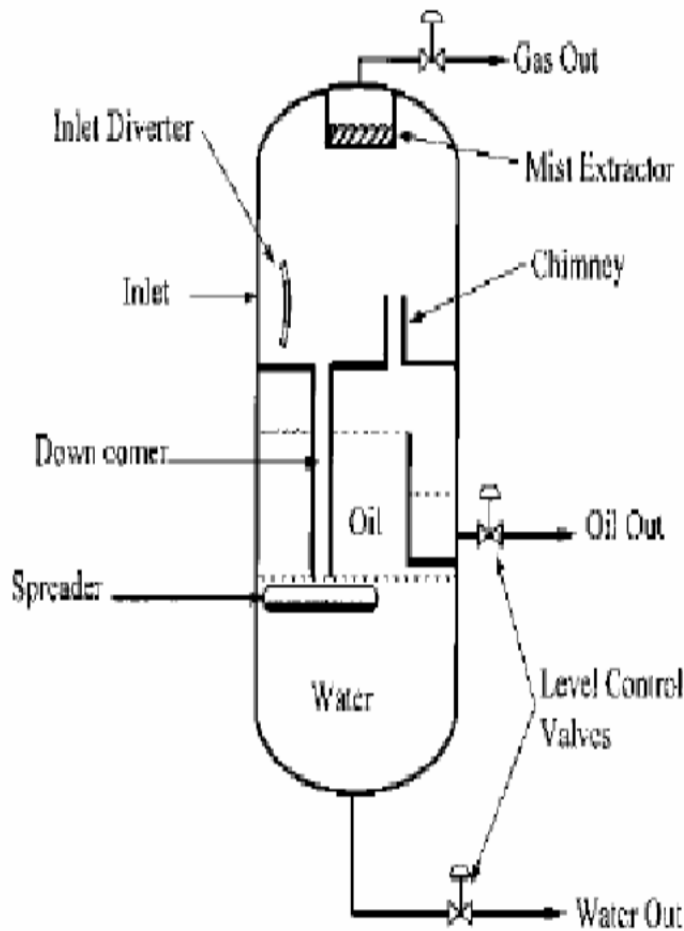


Figure 2: Vertical three phase separator  
Adapted from (Mokhatab and Poe, 2012)

### 2.3 Deliquidizer

The deliquidizer is one of the units in the separation system discussed that is compact and based on the inline technology as briefly discussed in section 1 above. The role of the deliquidizer is to separate liquid from the gas stream from the gravity separator where bulk separation takes place. The components of a typical deliquidizer are shown in the figure 3 below. The figure is adapted from link here

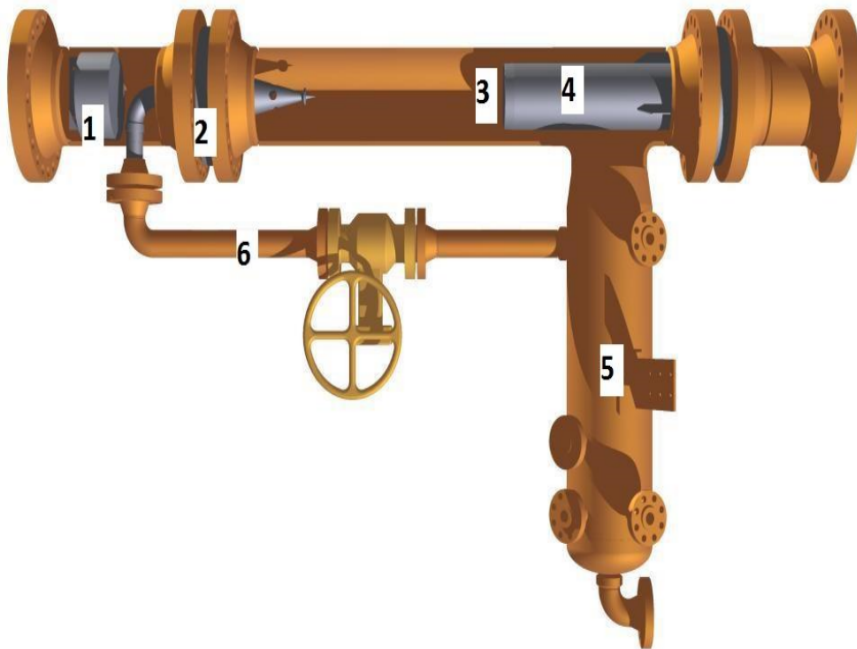


Figure 3: Typical inline deliquidizer

The multiphase flow stream enters the unit through a flow conditioning element(1) which equally distributes the liquid droplets throughout the pipe cross sectional area. The stationary swirl element(2) then brings the two phase mixture into rotation which causes the two phases to separate because of their difference in densities. The liquid creates a thin film on the

pipe's outer wall and the gas exits through a small pipe in the center of the main pipe(3) (Hamoud et al., 2009). The liquid enters the annular space between the two pipes, hits the back wall of the deliquidizer and enters the boot section(5). This liquid carries some gas and the latter is removed and recycled back through the recycle line(6). The liquid is discharged at the bottom of the boot section. The gas outlet pipe(4) has an anti-swirl element which stops the rotation, resulting in a low-total pressure drop across the deliquidizer. The control of the deliquidizer will only require level control for the liquid from the boot section (Hamoud et al., 2009).

## 2.4 Degasser

The role of the degasser in the compact separation system here discussed is to separate gas from the liquid stream from the gravity separator after bulk separation. This is also a compact unit based on the inline technology.

As can be seen from figure 4, the liquid dominated gas liquid stream in this case from the gravity separator enters the unit and is forced into rotation by the swirl element near the entrance. The rotation of the mixture stream enhances separation of the phases with the gas core forming in the centre of the unit (FMCtechnologies, 2011). The gas core then enters the smaller diameter pipe in the centre of the degasser and is discharged to the deliquidizer while the gas free-liquid continues to the exit of the unit and to the pump.

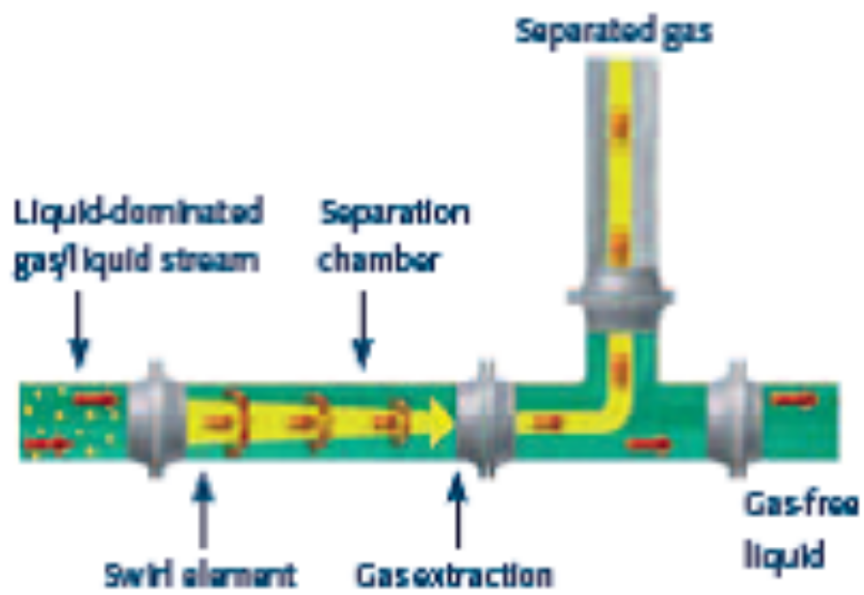


Figure 4: Typical inline degasser  
Adapted from (FMCtechnologies, 2011)

### 3 MODELLING OF THE DELIQUIDIZER

The modelling of the deliquidizer is to be done in two parts, namely modelling the separation of the liquid droplets from the gas stream in the first section of the deliquidizer (called the main deliquidizer section in this report) and the separation of the gas bubbles from the separated liquid stream that enters the second section of the deliquidizer (the boot section).

It's extremely important to state that some if not most of the concepts used for modelling in the following subsections are normally applied in particle technology but have been assumed here to as well as apply to droplet separation.

#### 3.1 Modelling of separation in the main deliquidizer section

In this section, cyclonic separation is considered where the forces present push the heavier liquid phase outwards to the wall while the lighter gas phase remains in the middle section. The forces generated are greater than the gravity forces used in conventional separators.

##### 3.1.1 Radial velocity

A drag force is exerted on the liquid droplets entrained in the gas phase. For the separation of the liquid droplets to take place, the external force applied on the droplets must exceed the drag force. The most basic force applied is the gravitational force . For the droplet to separate, the gravitational force minus the bouyancy force must equal the drag force (Monsen, 2012). Therefore a force balance gives,

$$(\rho_l - \rho_g)gV_p = F_D \quad (1)$$

where  $\rho_l$  is the density of the liquid,  $\rho_g$  is the density of the gas,  $V_p$  is the volume of the droplet,  $g$  is the gravitation constant and  $F_D$  is the drag force.

The drag force  $F_D$  is based on stoke's law, considering the droplet to be spherical and of a small diameter (Stene, 2013). Then,

$$F_D = 3\pi U_t d_p \mu_g = 6\pi U_t r_p \mu_g \quad (2)$$

where  $U_t$  is the droplet terminal velocity,  $d_p$  and  $r_p$  are the droplet diameter and radius respectively,  $\mu_g$  is the gas viscosity. Therefore substituting for  $F_D$  in equation 1 gives,

$$(\rho_l - \rho_g)gV_p = 6\pi U_t r_p \mu_g \quad (3)$$

Substituting for  $V_p = \frac{4}{3}\pi r_p^3$  in equation 3 and making  $U_t$  the subject gives,

$$U_t = \frac{2(\rho_l - \rho_g)gr_p^2}{9\mu_g} = \frac{(\rho_l - \rho_g)gd_p^2}{18\mu_g} \quad (4)$$

The above terminal velocity equation represents the stable velocity the droplet reaches after an acceleration period in gas flow. The dependance of the terminal velocity on the droplet diameter results in the fact that smaller droplets attain their terminal velocity after a short time period than larger droplets (Stene, 2013).

With a closer look at equation 4, you note that the external force here involved is the gravitational force. However, for cyclonic separation, there are centrifugal forces, thus the centripetal acceleration  $a_c$  which is assumed to have a greater influence on the droplet than gravity replaces the gravitational acceleration  $g$  in the above equation (Stene, 2013). The centripetal acceleration  $a_c$  is given by  $a_c = \frac{u_t^2}{r}$  where  $u_t$  is the tangential velocity and  $r$  the radial position.

In a cylindrical geometry, equation 4 can now be written as;

$$u_r = \frac{dr}{dt} = \frac{(\rho_l - \rho_g)d_p^2 u_t^2}{18\mu_g r} \quad (5)$$

The swirl flow in the deliquidizer is in this case considered as a forced vortex flow, which is swirling flow with the same tangential velocity distribution as a rotating solid body as opposed to free vortex flow, the way a

frictionless fluid would swirl. This is done for simplicity as the tangential velocity distribution for real swirling flows is intermediate between these two extreme cases (Hoffmann and Stein, 2002). For a forced vortex flow, the tangential velocity  $u_t$  is given by  $u_t = \omega r$  where  $\omega$  is the angular velocity measured in radians per unit of time and is a constant for a forced vortex flow (Hoffmann and Stein, 2002). Substituting for  $u_t$  in equation 5 gives

$$u_r = \frac{dr}{dt} = \frac{(\rho_l - \rho_g)d_p^2\omega^2 r}{18\mu_g} \quad (6)$$

### 3.1.2 Time of flight model

Let us now focus on the time of flight model, a comparison of the time required by the droplet that enters at a certain inlet position to reach the cyclone wall to the time available to traverse the length of the cyclone (Hoffmann and Stein, 2002).

Figure 5 illustrates how the radial velocity affects the droplet trajectory. The gas entrained with liquid droplets enters the separator and is set into circular motion. The centrifugal and drag forces cause the radial velocity of the droplet to increase resulting in an arced trajectory (Monsen, 2012).

Assuming that a droplet enters at an inlet position  $r_l$ , where  $r_l$  is the distance from the its inlet position to the centrifuge centre, the time  $t_{radial}$  for the droplet to reach the centrifuge wall  $R$  can be obtained by integration of equation 6 from  $r_l$  to  $R$  (Monsen, 2012). This gives;

$$t_{radial} = \frac{18\mu_g}{(\rho_l - \rho_g)d_p^2\omega^2} \ln \frac{R}{r_l} \quad (7)$$

On the other hand, the time  $t_{axial}$  available for the droplet from the inlet to exit of the centrifuge is given by;

$$t_{axial} = \frac{L}{v_z} = \frac{\pi R^2 L}{Q_i} \quad (8)$$

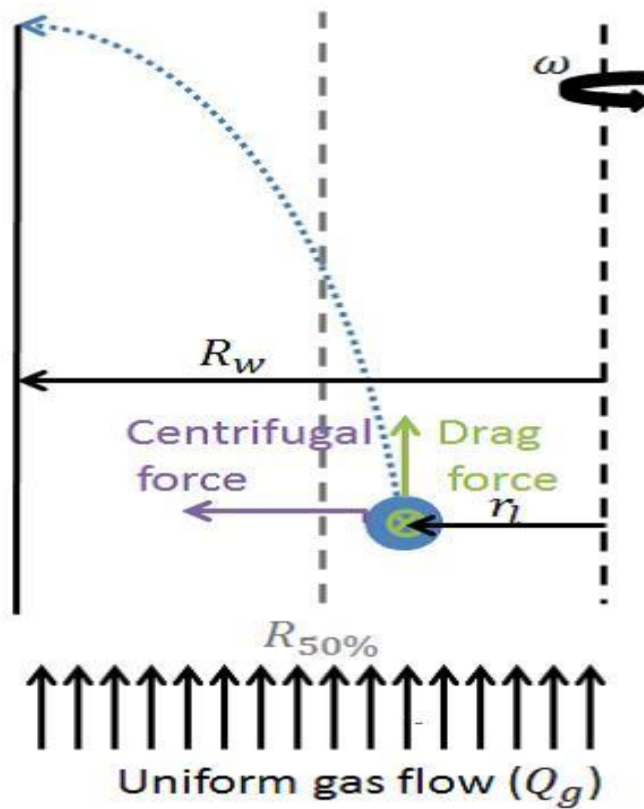


Figure 5: Trajectory of droplet experiencing a centrifugal force  
 Adapted from (Monsen, 2012)

where  $L$  is the length of the centrifuge,  $v_z$  is the axial velocity and  $Q_i$  is the inlet volumetric flow rate.

A comparison of  $t_{radial}$  and  $t_{axial}$  leads to possible cases. Either  $t_{radial}$  is less than  $t_{axial}$ , implying that the liquid droplet will reach the wall before exiting the separator thus separating from gas flow. Or  $t_{radial}$  is greater than  $t_{axial}$ , implying that the liquid droplet will not reach the wall of the separator and remains entrained in the gas flow (Monsen, 2012).

Based on this analysis, it's possible to find the liquid droplet entrance position  $r_l$  above which all the liquid droplets are separated if they are of the same diameter  $d_p$  and are uniformly distributed across the cross-sectional area of the separator, if the diameter  $d_p$  and the angular velocity  $\omega$  are known or can be estimated.

These two are basic assumptions that are used for the model being developed for separation of liquid droplets from the gas phase in the deliquidizer. Therefore, equating the two expressions for  $t_{radial}$  and  $t_{axial}$ , it is possible to find the position  $r_l$ . Thus;

$$\frac{18\mu_g}{(\rho_l - \rho_g)d_p^2\omega^2} \ln \frac{R}{r_l} = \frac{\pi R^2 L}{Q_i} \quad (9)$$

Making  $r_l$  the subject gives;

$$r_l = \exp\left(\ln R - \frac{(\rho_l - \rho_g)d_p^2\omega^2\pi R^2 L}{18\mu_g Q_i}\right) \quad (10)$$

$$r_l = \exp\left(\ln R - \frac{(\rho_l - \rho_g)d_p^2\omega^2 t_{axial}}{18\mu_g}\right) \quad (11)$$

It's quite obvious from equation 10 that  $r_l$  is dependent on the inlet volumetric flow rate  $Q_i$ , angular velocity  $\omega$ , droplet diameter  $d_p$ , density difference between the phases to be separated  $\rho_l - \rho_g$ , viscosity of the continuous phase  $\mu_g$  and the length  $L$  and radius  $R$  of the separator.

### 3.1.3 Uniform droplet distribution

Let us focus once again on the assumption of uniform droplet distribution of liquid phase. It's assumed in this model that all the liquid is dispersed into droplets of a certain size, diameter  $d_p$  that are distributed uniformly into the gas phase. This assumption is supported by the fact that there is a mixing element at the start of the deliquidizer whose role is to equally distribute the liquid droplets throughout the pipe cross sectional area. Refer to subsection 2.3 for the deliquidizer functioning.

Let  $n$  be the total number of droplets entering the unit. The number of droplets per unit cross sectional area  $n_a = \frac{n}{\pi R^2}$ . The number of droplets separated  $n_{sep}$  (with  $t_{radial}$  less than  $t_{axial}$ ) are in the cross sectional area  $\pi(R^2 - r_l^2)$ . Thus  $n_{sep} = n_a\pi(R^2 - r_l^2) = n(1 - (\frac{r_l}{R})^2)$ .

Therefore, volume separated  $V_{sep} = n(1 - (\frac{r_l}{R})^2)V_p$  where  $V_p = \frac{4}{3}\pi r_p^3$  is the volume of each droplet. But  $nV_p$  is the total volume of liquid into the separator. Therefore the volumetric flow rate of liquid separated  $\dot{V}_{sep} = \dot{V}_{liq-in}(1 - (\frac{r_l}{R})^2)$  where  $\dot{V}_{liq-in}$  is the volumetric flow rate of liquid into the separator. If  $Q_i$  is the total inlet volumetric flow rate and  $f$  is the gas volume fraction, then  $\dot{V}_{liq-in} = (1 - f)Q_i$ . Therefore,  $\dot{V}_{sep}$  is given by;

$$\dot{V}_{sep} = (1 - f)Q_i(1 - (\frac{r_l}{R})^2) \quad (12)$$

The equation 12 predicts the volumetric flow rate of liquid separated from the gas phase in the deliquidizer. Note that  $r_l$  is dependent on other parameters as previously discussed in this subsection. Therefore, the volumetric flow rate of liquid separated  $\dot{V}_{sep}$  is similarly dependent on the same parameters.

### 3.1.4 Gas volume fraction

Finally, the gas volume fraction  $\alpha_g$  of the exiting stream after separation of the liquid is approximated as follows;

$\alpha_g = \frac{\text{total.vol.of.gas.in} - \text{vol.of.gas.to.boot}}{\text{total.vol.in} - \text{vol.of.liq.separated}}$  Assuming that the volume of gas to boot section with liquid is far smaller than the total gas volume into the separator, then;  $\alpha_g = \frac{\text{total.vol.of.gas.in}}{\text{total.vol.in} - \text{vol.of.liq.separated}}$ . Thus  $\alpha_g$  is given by;

$$\alpha_g = \frac{fQ_i}{Q_i - \dot{V}_{sep}} \quad (13)$$

Assuming that the angular velocity  $\omega$  is some function of the total inlet volumetric flow rate  $Q_i$  and therefore known, equations 8,11,12 and 13 are the model equations that have been used for the modelling the separation. They are summarised as follows;

$$t_{axial} = \frac{L}{v_z} = \frac{\pi R^2 L}{Q_i}$$

$$r_l = \exp\left(\ln R - \frac{(\rho_l - \rho_g)d_p^2 \omega^2 t_{axial}}{18\mu_g}\right)$$

$$\dot{V}_{sep} = (1 - f)Q_i\left(1 - \left(\frac{r_l}{R}\right)^2\right)$$

$$\alpha_g = \frac{fQ_i}{Q_i - \dot{V}_{sep}}$$

## 3.2 Concepts for model improvement

The concepts in sub subsections 3.2.1, 3.2.2 and 3.2.3 are presented because they could be useful in improving the model discussed in subsection 3.1.

### 3.2.1 Modelling of swirl with decay

The concepts in this sub subsection 3.2.1 are for an axial cyclone which operates in a manner similar to the deliquidizer.

The radial migration velocity is given in (van Wissen et al., 2007) as given by equation 5 in subsection 3.1. The strength of the swirling motion

decays as a result of wall friction resulting in an axial decay of the tangential velocity. Assuming that the tangential velocity  $u_t$  is constant with respect to  $r$ , the axial decay is given by an exponential function according to experimental observations as follows (van Wissen et al., 2007).

$$u_t = u_{t0} \exp\left(-\frac{z}{R}\beta\right) \quad (14)$$

Here  $u_{t0}$  is the tangential velocity at the point where the swirl is initiated,  $z$  is the axial distance and  $\beta$  an empirical factor about 0.05.

Assuming once again that the axial velocity  $u_a$  of the carrier fluid (gas in this case) is constant with respect to  $r$ ,  $u_a = u_{a0}$  (van Wissen et al., 2007). The axial position of the droplet is given by  $dz/dt = u_{a0}$  which yields  $z = u_{a0}t$  upon integration.

Substituting for  $z$  in equation 14 and substituting the resultant equation for  $u_t$  into equation 5 for the tangential velocity gives;

$$u_r = \frac{dr}{dt} = \frac{(\rho_l - \rho_g)d_p^2 u_{t0}^2 \exp\left(-\frac{u_{a0}t}{R}\beta\right)}{18\mu_g r} \quad (15)$$

Here  $\beta = 0.1$

Thus;

$$r \frac{dr}{dt} = \frac{(\rho_l - \rho_g)d_p^2 u_{t0}^2 \exp\left(-\frac{u_{a0}t}{R}\beta\right)}{18\mu_g} \quad (16)$$

The radial position  $r(t)$  of the droplet at any time  $t$  can be obtained by integration of equation 16 with respect to time  $t$ . This gives;

$$r^2(t) = \frac{2(\rho_l - \rho_g)d_p^2 u_{t0}^2}{18\mu_g} \left[ \frac{R}{\beta u_{a0}} \left( -\exp\left(-\beta \frac{u_{a0}}{R}t\right) + 1 \right) \right] + r^2(0) \quad (17)$$

where  $r(0)$  is the radial position of the droplet at  $t = 0$  (entrance).

### 3.2.2 Energy consumption

The energy consumption in a cyclone is as a result of the pressure drop undergone by the fluid flowing through the cyclone. The total energy loss

is obtained by integration as follows (van Wissen et al., 2007);

$$\dot{E} = \int_0^{2\pi} \int_0^R \rho_f u_{t0}^2 u_a r dr d\theta$$

where  $\rho_f$  is the density of the carrier fluid. Note that  $u_{t0}$  and  $u_a$  were considered constant with respect to  $r$ . Therefore, integration yields  $\dot{E} = \pi R^2 \rho_f u_{t0}^2 u_a = \rho_f u_{t0}^2 Q$  where  $Q$  is the volumetric flow rate given by  $Q = \pi R^2 u_a$ .

The specific energy consumption  $\varepsilon$  (energy consumption per unit mass) is thus;  $\varepsilon = \frac{\dot{E}}{\rho_f Q} = u_{t0}^2$  (van Wissen et al., 2007).

Finally, the pressure drop over the cyclone is given by;

$$\Delta P = \varepsilon \rho_f = \rho_f u_{t0}^2 \quad (18)$$

### 3.2.3 Re-entrainment

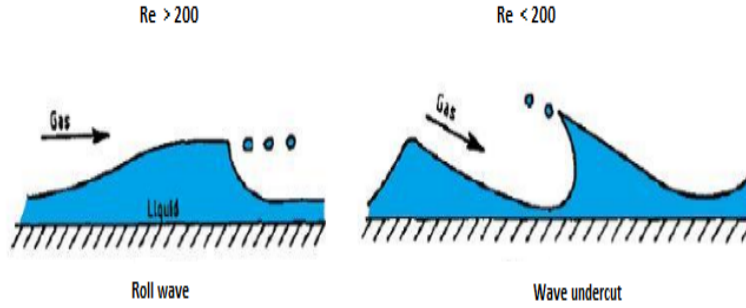


Figure 6: Re-entrainment mechanisms

Adapted from (Monsen, 2012)

According to (Swanborn, 1988), the breakup of the liquid film formed by separated droplets is supposed to be the major source of re-entrainment if the maximum capacity of the separator is exceeded. The principal mechanisms

responsible for film breakup are roll waves and wave undercut as shown in figure 6.

Roll waves are considered to appear for thick films and at high liquid film Reynolds numbers. The shape and movement of a roll wave is determined by the surface tension and hydrodynamic forces, and numerous small drops are formed by an extreme deformation of the top of the wave under certain condition (Swanborn, 1988).

Wave undercut on the other hand is not often encountered but takes place at only low liquid film Reynolds numbers and can take place without the occurrence of roll waves. This takes place at a certain gas and liquid velocity where the gas starts to cut the wave which starts to bulge, and can eventually burst by high pressure inside the half closed bubble forming droplets. These droplets can be projected at high radial velocities.

Let us now focus a bit on the different regimes for re-entrainment occurrence.

As can be seen from figure 7, there are three different regimes;

1. Minimum Reynolds number regime; this represents the minimal liquid film Reynolds number under which no re-entrainment will occur, irrespective of the gas velocity.
2. Rough turbulent regime; which is attached to a certain gas velocity above which re-entrainment of a liquid film occurs (irrespective of its Reynolds number).
3. Transition regime; which connects the regimes described above.

Separate correlations have been developed to describe the effect of these regimes on re-entrainment but unfortunately, no more than this can be presented at this moment.

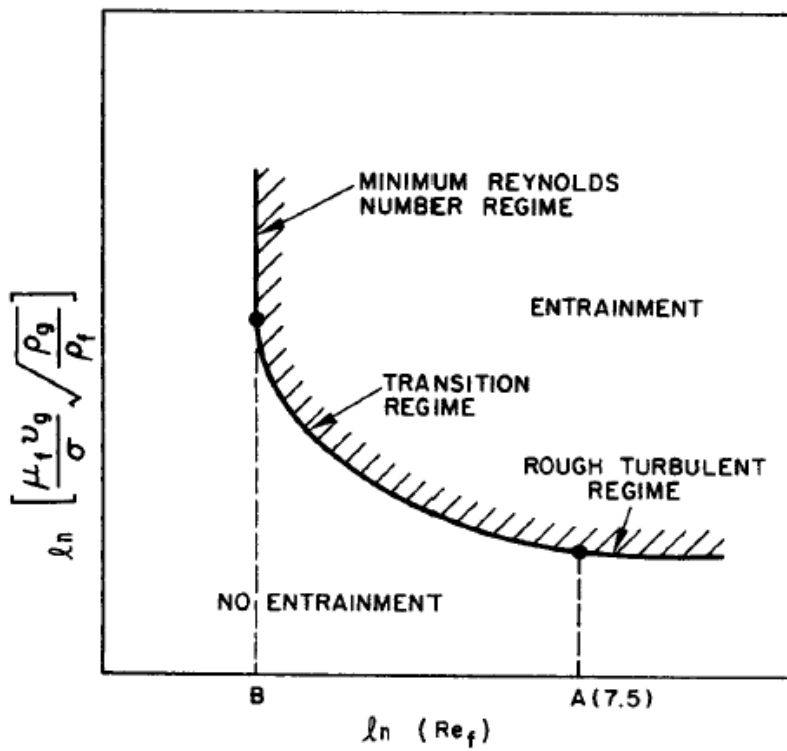


Figure 7: Occurrence of re-entrainment

Adapted from (Swanborn, 1988)

## 4 RESULTS AND DISCUSSION

Note once again that assuming the angular velocity  $\omega$  is some function of the total inlet volumetric flow rate  $Q_i$  and therefore known (since the inlet flow rate determines the swirl strength), equations 8,11,12 and 13 are the model equations that have been used for the modelling the separation in the main deliquidizer section.

We have assumed some functions of  $\omega$  against  $Q_i$  and used the model equations above to obtain the results that are presented in this section. This has been done in Matlab and the scripts are found in the Appendix. Script `gasfraction.m` is used to obtain the results in figures 8, 9, 10 and 11 for each  $\omega$  function. Script `gasnew.m` is used to obtain the results in figures 13 and 14.

The table 1 shows the parameters used for the Matlab scripts.

Table 1: Parameters

Parameters	value	unit
$\rho_g$	15.7	$kg/m^3$
$\rho_l$	850	$kg/m^3$
$L$	1.5	$m$
$R$	0.075	$m$
$d_p$	150	$\mu m$
$\mu_g$	$1.83 * 10^{-5}$	$Pa s$
$f$	0.82	—

The figures 8 and 9 show functions of  $\omega$  against  $Q_i$  used to obtained the model results shown in figures 10,11 and 13. These model results have been compared to data in the same plots. For figure 14, the two functions were corrected so that model results are close to the data.

The two functions are;

1. Power function; the function used is  $\omega = 0.01 * Q_i^{1.37}$
2. Gompertz function; used is  $\omega = 5 * \exp(-9 * \exp(-0.05 * (Q_i)))$

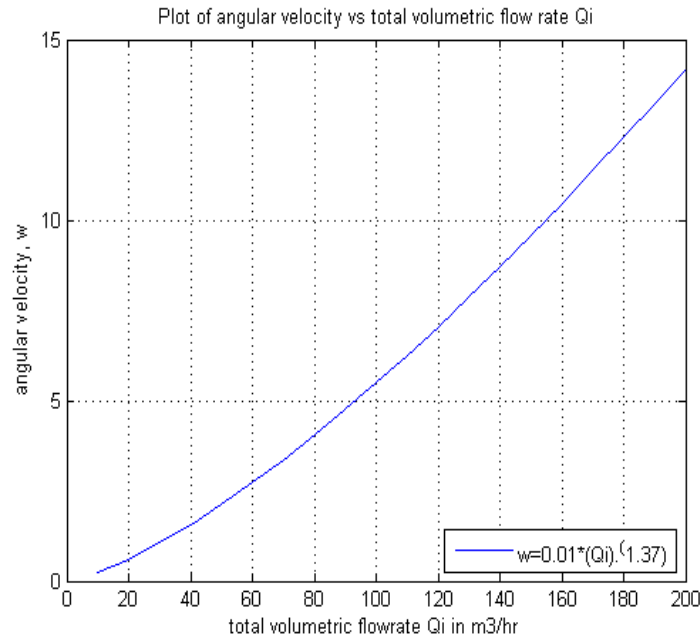


Figure 8: Power function of  $w$  against  $Q_i$

As is seen in figure 10, the prediction of model results by the power function is relatively okay for the data obtained when the flow rates  $Q_i$  are less than  $100 \text{ m}^3/\text{hr}$  but fails horribly above about  $100 \text{ m}^3/\text{hr}$ . This is due to the fact that above the maximum, probably the estimation of  $\omega$  by the function in this region is too large producing larger estimations of the gas volume fraction than expected. Probably, this decrease in the quality of the gas volume fraction thought to be as a result of re-entrainment of the separated liquid back to the gas phase might also be another reason since the model does not cater for re-entrainment.

On the other hand, the prediction of model results by the Gompertz function on average does relatively better than using the power function as can be observed from figure 11. This might be due to the fact that angular

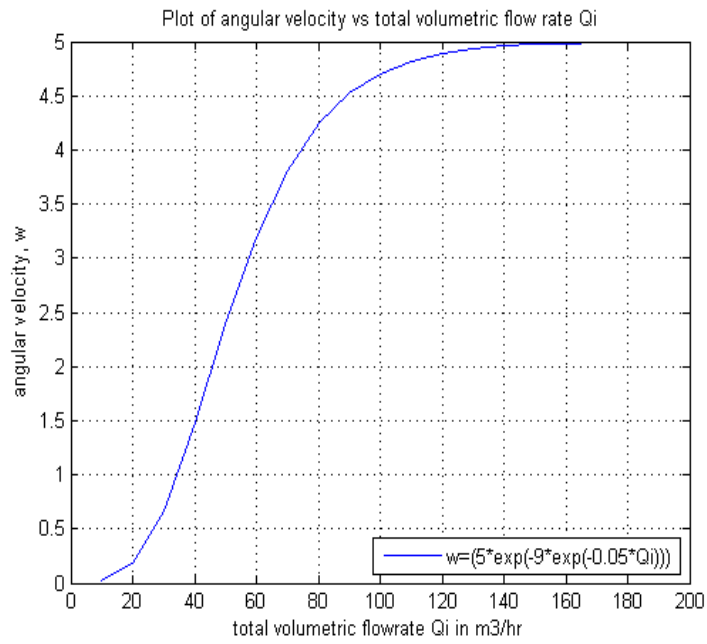


Figure 9: Gompertz function of  $w$  against  $Q_i$

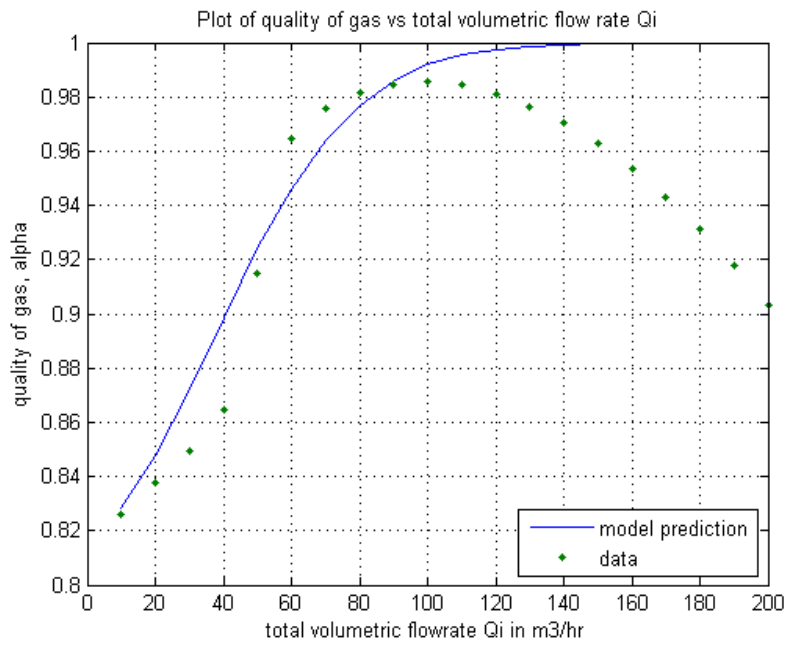


Figure 10: Model results for Power function

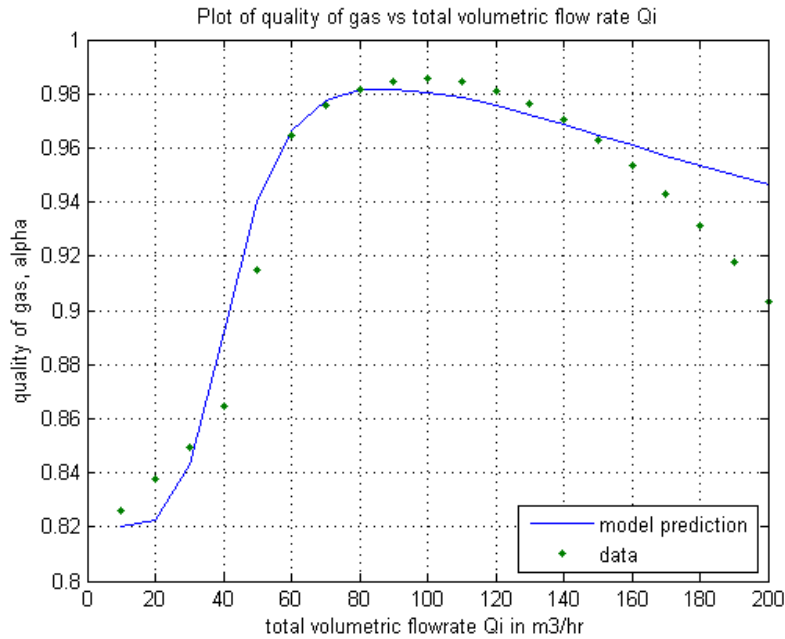


Figure 11: Model results for Gompertz function

velocity prediction by the Gompertz function is slowest at the start and the end. However, the model prediction is poor at high flow rates close to above  $160 \text{ m}^3/\text{hr}$  and this is thought to be probably due to overestimation of the angular velocity or because the model used does not cater for re-entrainment. Therefore, failure of the model is thought to be due to overestimation of the angular velocities or failure to cater for cater for re-entrainment at high inlet flow rates.

For figures 13 and 14, a different set of masked data obtained is used for comparison to model results. This data is shown in the figure 12.

However, its worth of mention that the total inlet volumetric flow rates used in this second data set for comparison are distributed closer to data that gives the maximum gas volume fractions as seen in figures 10 and 11.

In figure 13, the model-1 and model-2 results shown are respectively the predicted results by the same power and Gompertz functions used pre-

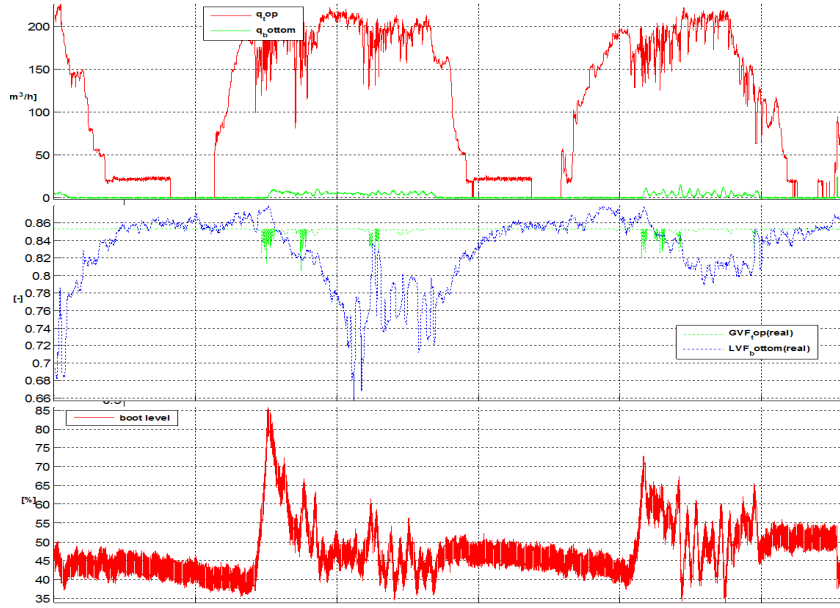


Figure 12: Masked data for comparison

viously. It is evident in this figure that the prediction by the model is relatively higher than expected as per these results. In fact model-1 predicts gas volume fractions of 1 which is 100% separation efficiency which is practically impossible. But this indicates that the angular velocities used are far higher than those that could possibly be generated in reality by the inlet volumetric flow rates.

Bearing this in mind, corrections on the angular velocities were made by altering the coefficients in the power and Gompertz functions. The following two functions were used to obtain model-1 and model-2 results shown in 14.

1. Power function; the function used is  $\omega = 0.01 * Q_i$
2. Gompertz function; used is  $\omega = 2.2 * \exp(-9 * \exp(-0.025 * (Q_i)))$

The predictions by the model are now much better than in the previous case.

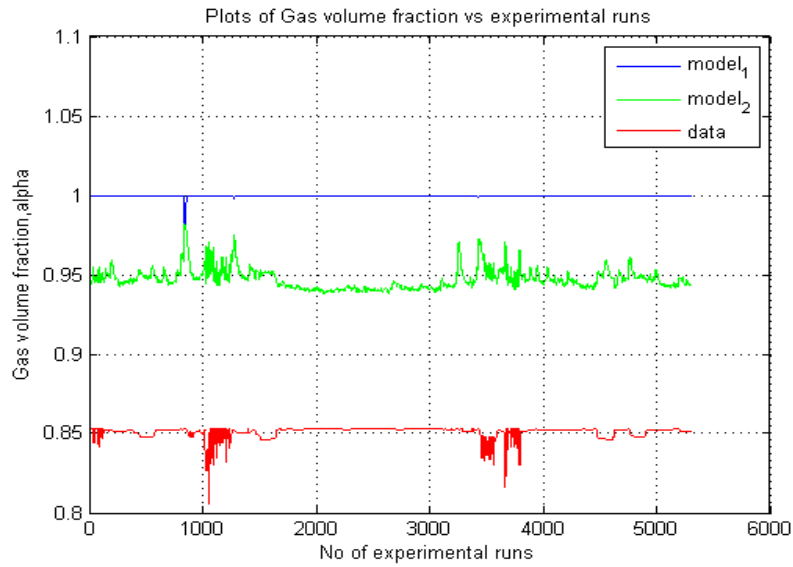


Figure 13: Comparison of model results to data

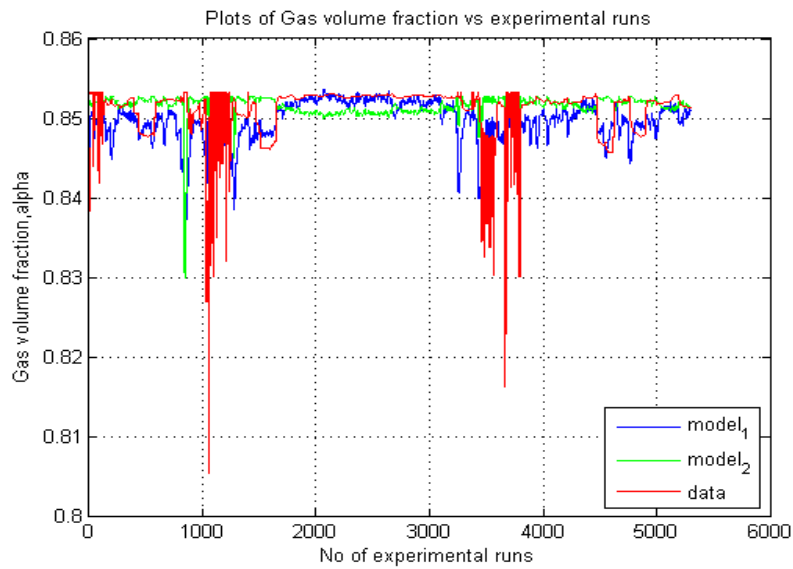


Figure 14: Comparison for corrected angular velocities

## 5 CONCLUSION AND FUTURE WORK

### 5.1 Conclusion

It has been shown in the section 4 that the model developed in this report performs averagely well in predicting separation of liquid from the gas phase in the main section of the deliquidizer.

However, there are some short comings of the model that inhibit the accuracy of it's predicted results. The model is generally identified not to cater for re-entrainment of separated liquid back to gas, a phenomena thought to occur at high flow rates probably as a result of turbulence. The other short coming is to determine how the angular velocity  $\omega$  depends on the total inlet volumetric flow rates. In this report, we assumed the dependence as power and Gompertz functions, and the results obtained though both encouraging did not clearly indicate which is better for both of the data sets used for comparison.

In conclusion, despite the short comings, the model seems to give promising results, and with some model improvements as noted, better performance is expected.

### 5.2 Future work

Model improvement by incorporating the concept of re-entrainment or using a function of angular velocity against volumetric flow rate that increases to a maximum and starts decreasing so as to mimic the physical behaviour of the gas volume fraction dependence on volumetric flow rate.

Modelling of separation of gas from the liquid stream that goes into the boot section and prediction of the quality of liquid out of the bottom of the boot section.

Modelling of separation in the gravity separator and degasser, and steady state simulation of the compact separation system.

Optimization of the compact separation system with an operational objective of adjusting the available valves in such a way that the gas content in the liquid stream to the pump is minimized.

## Bibliography

- Alary, V., Marchais, F., Palermo, T., et al. (2000). Subsea water separation and injection: A solution for hydrates. In *Offshore Technology Conference*. Offshore Technology Conference.
- Ellingsen, C. (2007). Compact sub sea separation: Implementation and comparison of two different control structures. Master's thesis, Norwegian University of Science and Technology.
- FMCTechnologies (2011). Compact total separation systems.
- Hamoud, A. A., Boudi, A. A., and Al-Qahtani, S. D. (2009). New application of an inline separation technology in a real wet gas field. *SAUDI ARAMCO JOURNAL OF TECHNOLOGY*, page 41.
- Hoffmann, A. C. and Stein, L. E. (2002). Gas cyclones and swirl tubes. *Springer-Verlag Berlin Heidelberg*, 2008.
- Mokhatab, S. and Poe, W. A. (2012). *Handbook of natural gas transmission and processing*. Gulf Professional Publishing.
- Monsen, G. O. T. (2012). Modeling of a centrifugal separator for dispersed gas-liquid flows.
- Sayda, A. F. and Taylor, J. H. (2007). Modeling and control of three-phase gravilty separators in oil production facilities. In *American Control Conference, 2007. ACC'07*, pages 4847–4853. IEEE.
- Stene, M. (2013). Cfd study of a rotating gas-liquid separator: Design og bygging av flere mikro-dråpe generatorer.
- Swanborn, R. A. (1988). *A new approach to the design of gas-liquid separators for the oil industry*. Univerity of Delft.

van Wissen, R., Brouwers, J., and Golombok, M. (2007). In-line centrifugal separation of dispersed phases. *AIChE journal*, 53(2):374–380.

## A Appendix

### A.1 gasfraction.m

```
% gasfraction.m
% This script is for the model developed for the deliquidizer
%section excluding the boot section
clc
clear all

% Parameters
rho_g=15.7; % density of gas corrected to 25 bar.
mu_g=1.83e-05; % viscosity of gas
rho_l=850; % density of liquid
R=7.5e-02; % radius of deliquidizer
L=1.5;% length of deliquidizer
f=0.82; % fraction of gas in inlet total stream
dp=150*1e-06; % droplet diameter

% Inputs
Qi=(10:10:200);% tot volumetric flowrate in m3/hr
vdot=(Qi)/3600;% in m3/s
w=(5*exp(-9*exp(-0.05*Qi)));% Gompertz function
%w=0.01*(Qi).^1.37 % Power function

% Model equations
t_axial= (pi*R^2*L)./vdot;
y=(log(R)-(t_axial*(dp^2)*(rho_l-rho_g).*(w.^2))/(18*(mu_g)));
% The radius above which we have separation is determined
%for all cases of omega
r_l=exp(y);
% Then determine the vol flow rate of separated liquid
vdot_sep=(1-f)*vdot.*(1-(r_l/R).^2);
% compute the gas volume fraction
alpha=(f*vdot)./(vdot-vdot_sep);
```

```

% Plotting
figure(1)
plot(Qi,w)
title('Plot of angular velocity vs total volumetric flow rate Qi')
xlabel('total volumetric flowrate Qi in m3/hr')
ylabel('angular velocity, w')
legend('w=(5*exp(-9*exp(-0.05*Qi)))','Location','SouthEast')
grid

figure(gcf+1)
plot(Qi,alpha)
title('Plot of quality of gas vs total volumetric flow rate Qi')
xlabel('total volumetric flowrate Qi in m3/hr')
ylabel('quality of gas, alpha')
axis([0 200 0.8 1])
legend('model prediction','data','Location','SouthEast')
grid
hold on

% Comparison of model results to the data obtained
alpha_g=[0.826029947 0.837487521 0.849603948 0.8644 0.915...
0.9644 0.975596052 0.981712479 0.984770053 0.985498797...
0.98425603 0.981246559 0.9766 0.970404191 0.962721735...
0.953599005 0.943071424 0.931166734 0.917907113 0.903310604 ];

scatter(Qi,alpha_g, '.')

```

## A.2 gasnew.m

```
% gasnew script
clc
clear all

% Parameters
rho_g=15.7; % density of gas corrected to 25 bar.
mu_g=1.83e-05; % viscosity of gas
rho_l=850; % density of liquid
R=7.5e-02; % radius of deliquidizer
L=1.5;% length of deliquidizer
f=0.82; % fraction of gas in inlet total stream
dp=150*1e-06;

% Inputs
load data_new % experimental data results
vdot=(Qi)/3600;
w=0.01*(Qi);
%w=0.01*(Qi).^1.37 % Power function used in first case

% Model
t_axial= (pi*R^2*L)./vdot;
y=(log(R)-(t_axial*(dp^2)*(rho_l-rho_g).*(w.^2))/(18*(mu_g)));
r_l=exp(y);

% Then determine the vol flow rate of separated liquid
vdot_sep=(1-f)*vdot.*(1-(r_l/R).^2);

% compute the gas volume fraction
alpha=(f*vdot)./(vdot-vdot_sep);

% Plotting
figure(1)
plot(alpha)
```

```

hold on

w=(2.2*exp(-9*exp(-0.025*Qi)));
%w=(5*exp(-9*exp(-0.05*Qi)));% Gompertz fnc used in first case
t_axial= (pi*R^2*L)./vdot;

y=(log(R)-(t_axial*(dp^2)*(rho_l-rho_g).*(w.^2))/(18*(mu_g)));

% The radius above which we have separation is
determined for all cases of omega
r_l=exp(y);
vdot_sep=(1-f)*vdot.*(1-(r_l/R).^2);

% compute the gas volume fraction
alpha=(f*vdot)./(vdot-vdot_sep);

plot(alpha,'green')
hold on
plot(Gvf_top,'red')
title('Plots of Gas volume fraction vs experimental runs')
xlabel('No of experimental runs')
ylabel('Gas volume fraction,alpha')
legend('model.1','model.2','data','Location','SouthEast')
grid on

```